Intra-conduction-band magneto-optical studies of InSb

M. W. Goodwin* and D. G. Seiler
Center for Applied Quantum Electronics, Department of Physics, North Texas State University, Denton, Texas 76203
(Received 3 September 1982)

CO_2-laser—induced phonon-assisted cyclotron-resonance harmonics (PACRH) in n-type InSb are investigated at low magnetic fields with photoconductivity techniques. The high resolution allowed transitions up to the 23rd harmonic to be seen. Polarization studies of PACRH show that strong resonances are present for $\vec{e}\perp\vec{B}$ (but not for $\vec{e}||\vec{B}$) in the Voigt geometry. In the Faraday geometry, the resonances were found to be of approximately equal amplitude for both σ_R and σ_L circularly polarized light. A large variety of intra-conduction-band magneto-optical experimental work has been unified and explained using a modified Pidgeon-Brown energy-band model and only one set of band parameters. These include cyclotron resonance, combined resonance, cyclotron-resonance harmonics, combined resonance harmonics, electron-spin resonance, and PACRH data from a wide variety of authors. The resulting set of energy-band parameters are $E_g=235.2$ meV, $E_p=23.2$ eV, $\Delta=0.803$ eV, $\gamma_1=3.25$, $\gamma_2=-0.2$, $\gamma_3=0.9$, $\kappa=-1.3$, $F=-0.2$, $q=0.0$, $N_1=-0.55$. These parameters are also shown to explain the variation of the effective g factor with magnetic field. In addition, these parameters also quantitatively explain recent two-photon magnetoabsorption data and recent intra-valence-band data.

INTRODUCTION

Over the past several decades magneto-optical studies in semiconductors have proven capable of determining energy-band parameters because of the optical transitions that occur between magnetically quantized electronic or impurity states. The conduction band of InSb, in particular, has been extensively studied with a wide variety of techniques. In part this is because high-quality InSb material can be grown with a small number of impurities and excellent homogeneity characteristics. It is thus not surprising to find that a great many intra-conduction-band processes have been observed and studied in InSb. However, there have been few attempts to quantitatively characterize all these processes with theoretical models using the same set of energy-band parameters.

One purpose of this investigation is to unify the experimental work on the conduction band of InSb into a more logical and complete study. With a simplified 8×8 Pidgeon-Brown model[1] of the bands, we simultaneously explain a wide variety of conduction-band data: cyclotron resonance,[2–4] combined resonance,[2–7] cyclotron-resonance harmonics,[4–9] combined resonance harmonics,[4–9] electron-spin resonance,[10–12] and phonon-assisted cyclotron-resonance harmonics[4–7,13–15] (PACRH) using only one set of band parameters.

In past studies there has been limited success in explaining the magnetic field dependence of the conduction-band g factor of McCombe and Wagner[10] or the more recent results of Kuchar *et al.*[11] However, our new set of band parameters and calculations obtained here are shown to explain this magnetic field dependence extremely well. In addition we present new experimental work on PACRH. With a high-resolution CO_2-laser—induced photoconductivity technique, transitions up to the 23rd harmonic at very low magnetic fields ($\sim$ 6 kG) are resolved. From a polarization study of PACRH we find for the first time that the absorption strengths for the circularly polarized light configrations σ_R and σ_L are approximately equal in magnitude for the range of photon energies and magnetic fields in this study.

EXPERIMENTAL WORK

The method to obtain the new low-field data presented here on PACRH used the sensitive photoconductive response of the sample itself in conjunction with sampling oscilloscope and magnetic field modulation techniques. The source of incident radiation was a continuous-wave CO_2 laser with a tunable grating providing variable photon energies. The

laser beam was mechanically chopped, producing optical and hence photoconductivity pulses approximately 20 μsec wide at a repetition of 1200 Hz. The sample was mounted in an optical variable temperature Dewar between the pole faces of a 20-kG electromagnet. Helmholtz coils wrapped around the pole faces produced a 43-Hz, 400-G, peak-to-peak magnetic field modulation. A sampling oscilloscope and lock-in amplifier were used to process the photoconductivity pulses produced in the sample by the chopped laser beam and the ac magnetic field. The data were recorded as the second derivative of the photoinduced magnetoresistance (y axis) as a function of magnetic field (x axis).

The samples of n-type InSb were obtained from Cominco American, Inc. and had a net carrier concentration of $\sim 9\times 10^{13}$ cm^{-3} and an electron mobility of 700 000 cm/V sec at 77 K. The dimensions of the samples after cutting were approximately $6\times 2\times 0.2$ mm^3. After polishing on both sides with 3-μm alumina polishing grit, the samples were then etched in a bromine-methanol solution for about 1 min. Contacts to the samples were made by first fluxing the surface and then soldering small indium dots with small gold wires to the samples. Two end current contacts and two side voltage contacts formed a standard four-contact potential measuring geometry.

DISCUSSION OF THEORETICAL PROCESSES AND RESULTS

The theory of the Landau-level energies used in this study was based upon an 8×8 Pidgeon-Brown energy-band model developed by Pidgeon and Groves[16] and more recently[9,17] by Weiler *et al.* Weiler has reduced the full 8×8 Hamiltonian containing warping and inversion asymmetry effects to two 4×4 matrices (one each for the spin-up and spin-down Landau levels) which contain only warping effects along the diagonal part of the matrices. The reduced 4×4 Hamiltonians contain ten parameters which must be adjusted to fit the theoretical transition energies to a set of experimental data. Of these ten parameters a new one, N_1, was introduced by Weiler to include the spin-orbit splitting of higher bands of Γ_8 symmetry. The 4×4 matrices, which are solved numerically by a computer, give the energy eigenvalues for the conduction, valence (light and heavy hole), and spin-orbit split-off bands for both spin-up and spin-down Landau levels. The transition energies for the different magneto-optical processes are then calculated by combining the Landau-level energies with specific selection rules. In the following sections the selection rules for these different processes are given.

Cyclotron, combined, harmonics, and electron-spin resonances

Cyclotron resonance was first used by Dresselhaus *et al.*[18] to investigate the band structure of silicon and germanium. In simple terms, cyclotron resonance occurs when the energy between the $n=0$ and $n=1$ spin-up conduction-band Landau levels equals the incident photon energy. That is

$$\hbar\omega = E_a^c(1) - E_a^c(0), \tag{1}$$

where $\hbar\omega$ is the photon energy and $E_a^c(n)$ is the energy of the nth spin-up conduction-band Landau level. The defining equation for the cyclotron-resonance effective mass m_c^* is

$$\hbar\omega = \hbar\omega_c, \tag{2}$$

where $\omega_c = eB/m_c^*$, B is the magnetic field strength, and m_c^* is an effective mass which for conduction-band cyclotron resonance is an electron effective mass. This equation has been traditionally used for cyclotron resonance even for bands that are nonparabolic. Cyclotron resonance is a result of the selection rules $\Delta n = +1$; $\Delta s = 0$ for $\vec{e}\perp\vec{B}$ (σ_L polarization) and can be derived from one-photon absorption processes with the use of the usual spherical approximation.[9] When the magnetic field B is such that a resonance occurs, then electrons in the $n=0$ spin-up conduction-band Landau level will absorb photons from the optical flux and be excited to the $n=1$ spin-up conduction-band Landau level.

Cyclotron resonance in InSb was first observed in transmission studies by Dresselhaus *et al.*[19] using microwave radiation and later by Burstein *et al.*[20] using infrared radiation. Cyclotron resonance was also observed by a number of other investigators.[21–23] In addition to cyclotron resonance, McCombe and co-workers[2,3] studied other types of intra-conduction-band processes such as combined resonance, spin-down cyclotron resonance, and PACRH which will be discussed in the next section. Combined resonance is a process in which an electron initially in the $n=0$ spin-up conduction-band Landau level makes a transition by photon absorption to the $n=1$ spin-down Landau level. That is, at resonance

$$\hbar\omega = \hbar\omega_c + \hbar\omega_s = E_b^c(1) - E_a^c(0), \tag{3}$$

where $\hbar\omega_s$ is the energy between a spin-up and spin-down Landau level and

$$\hbar\omega_s = g_c^*\mu_B B, \tag{4}$$

where g_c^* is the Lande g factor and μ_B is the Bohr magneton. The selection rule for this process is again derived from the spherical approximation

treatment for one-photon absorption and is $\Delta n=+1$; $\Delta s=-1$ for $\vec{e}\|\vec{B}$ (π polarization).[9] This process is not allowed for $\vec{e}\perp\vec{B}$ in the spherical approximation. Spin-down cyclotron resonance obeys Eq. (2) except electron transitions occur between the spin-down ($s=-\frac{1}{2}$) levels of the $n=0$ and $n=1$ Landau levels. This effect is usually observed[2] at the higher temperatures (~ 77 K), where the tail of the probability distribution of carriers is long enough to significantly populate the higher-energy spin-down $n=0$ Landau level.

Another comprehensive study of conduction-band processes in InSb was performed by Johnson and Dickey.[4] In addition to those processes studied by McCombe, they observed resonant structure in transmission spectra which were caused by harmonics of cyclotron resonance. Harmonics of cyclotron resonance are the result of electrons in the spin-up $n=0$ Landau level being photoexcited to the spin-up state of some $n>1$ Landau level. Thus when a resonance condition occurs

$$\hbar\omega=n\hbar\omega_c=E_a^c(n)-E_a^c(0), \tag{5}$$

where $n=1$ is the condition for cyclotron resonance. It should be pointed out that because of nonparabolicity and quantum effects, the "harmonic" transitions $n\hbar\omega_c$ do not occur exactly at the energy n times $\hbar\omega_c$. Therefore, the notation $n\hbar\omega_c$ is used merely for labeling purposes. The origin of these processes in terms of selection rules cannot be derived in the usual spherical approximation. However, there have been extensive theoretical investigations[9,16,24] of these processes. Other processes which have also been observed in studies of the spin-flip Raman laser[25,26] are spin-flip with the harmonics of the cyclotron resonance or

$$\hbar\omega=n\hbar\omega_c+\hbar\omega_s=E_b^c(n)-E_a^c(0). \tag{6}$$

Electron-spin resonance associated with spin-flip processes can be described by

$$\hbar\omega=\hbar\omega_s=E_b^c(0)-E_a^c(0), \tag{7}$$

where electrons in the spin-up ($s=+\frac{1}{2}$) state are photoexcited to the spin-down ($s=-\frac{1}{2}$) state of the $n=0$ Landau level. Isaacson[27] and McCombe and Wagner[10] investigated this process in order to obtain the conduction-band g factor g_c^*, Eq. (4). More recently Kuchar *et al.*[11] found that the strength of the spin-resonance line depended upon the amount of uniaxial stress applied to the sample. However, the magnetic field positions of the resonances are not measurably effected. The magnitude of the observed g factor and its variation with magnetic field will be discussed in more detail later.

The band parameters used in this study were obtained by numerically fitting the theoretical transition energies to a large set of magneto-optical data. In addition to the intra-conduction-band data just discussed and PACRH data to be discussed later in this paper, a set of two-photon interband[28] and one-photon intra-valence-band[29] data were also used to numerically obtain the band-parameter set reported here. With all these processes the resulting band parameters reported here should be more uniquely determined than in previous studies.

Figure 1 shows the fit of the theoretical transition energies to the intra-conduction-band processes that have been described so far. The band parameters determined from the fit are $E_g=235.2$ meV, $E_p=23.2$ eV, $\Delta=0.803$ eV, $\gamma_1=3.25$, $\gamma_2=-0.2$, $\gamma_3=0.9$, $\kappa=-1.3$, $F=-0.2$, $q=0.0$, and $N_1=-0.55$. The definitions of these parameters are given by Weiler *et al.*[9] and a comparison with other work is reported by Littler *et al.*[29] It must be pointed out that our measurements could not satisfactorily determine the spin-orbit splitting energy Δ. We therefore used the value obtained by Aggarwal ($\Delta=0.803$ eV).[30]

In Fig. 1 are plotted the transition energy versus magnetic field data of several authors.[3–8] The data should represent most of the important work on the conduction band of InSb, but is not an exhaustive set. However, the data of other works[31,32] do agree with those results presented here. The labels correspond to the final state of the transition; the initial state for all the transitions is the spin-up $n=0$ or $a(0)$ Landau level. With this set of band parameters, a good fit to all the data is very apparent even to the high magnetic fields of 20.0 T (200 kG). At energies below 120 meV there is an excellent fit of the theoretical lines with the data. Above 120 meV for the $a(2)$, $b(2)$, and $a(3)$ transitions there does appear, however, to be a slight shift of the theory from the data. This may be the result of the energy-band model's failure to predict accurate transition energies at the higher energies. Another possibility might be that small adjustments in the band parameter set are needed to improve the fit. However, this deviation does not significantly detract from the good overall agreement of the theory with a large amount of data.

The data in Fig. 1 is a mixture of data obtained with B parallel to the $\langle 111\rangle$ and $\langle 100\rangle$ crystal directions. The theoretical lines were calculated for $\vec{B}\|\langle 100\rangle$ crystal direction. The data for the two crystal directions agree within experimental error, indicating no major differences between them. Figure 2 illustrates the differences in the theoretically calculated transition energies between the two directions with the band-parameter set given previously.

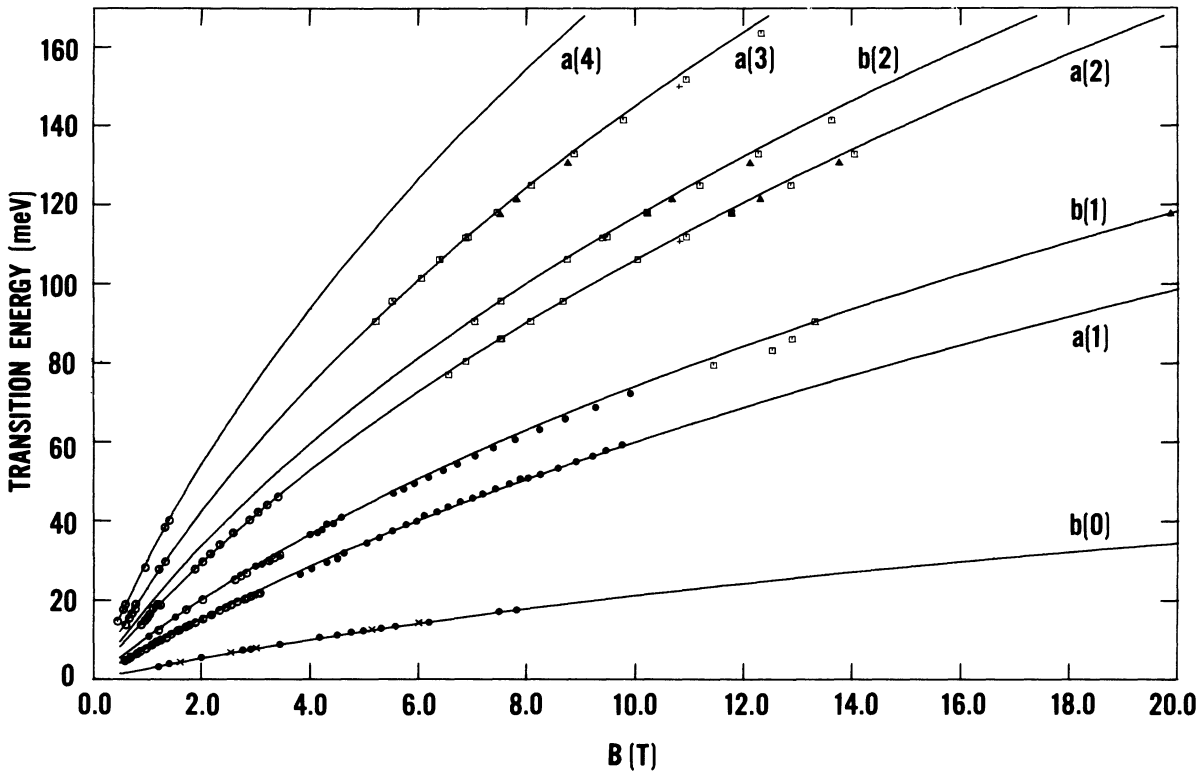

FIG. 1. Fan chart of various intraconduction processes used to determine the band parameter set of this study. The notation $a(n)$ or $b(n)$ refer to the final-state spin-up or spin-down level, respectively, of the nth Landau level. The data points are as follows: ●, Refs. 2 and 3; ×, Ref. 11; ○, Ref. 4; □, Ref. 5; ▲, Ref. 6; +, Ref. 8. The labels by the line represent electron spin resonances [$b(0)$], cyclotron resonance, [$a(1)$], combined resonance [$b(1)$], cyclotron resonance harmonics [$a(2)$, $a(3)$, $a(4)$], and combined resonance harmonics [$b(2)$].

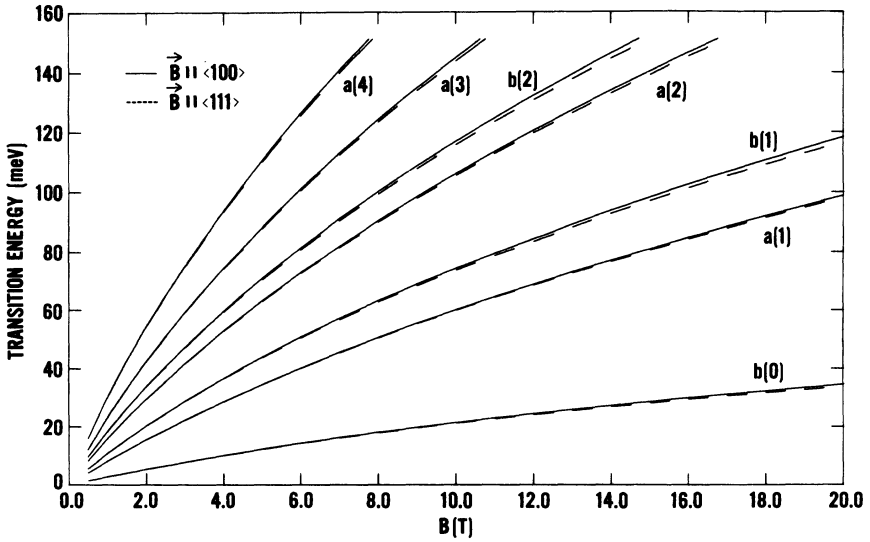

FIG. 2. Anisotropy differences for $\vec{B}||\langle 111\rangle$ and $\langle 100\rangle$ for the transitions in Fig. 1.

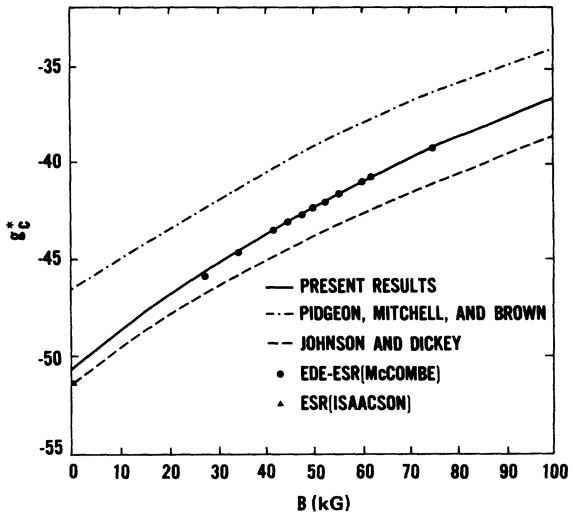

FIG. 3. Extrapolated magnetic field dependence of the conduction-band g_c^* factor showing the excellent fit of our theoretical calculations to the data of Refs. 3 and 27.

The $\vec{B}||\langle 111\rangle$ transition energies are only slightly lower in energy than the $\vec{B}||\langle 100\rangle$ transition energies, in agreement with the anisotropy measurements of McCombe.[33] The deviation is more pronounced for transitions at high energy and high magnetic fields. The high-field and high-energy data of Fig. 1 (□,▲) were obtained with $\vec{B}||\langle 100\rangle$, as were the theoretical lines, thus no discrepancy should exist because of the differences in the two crystal-field directions. There remain only the low-energy, low magnetic field data, which is a mixture of $\vec{B}||\langle 111\rangle$ and $\langle 100\rangle$ data and for which there should be no noticeable differences in energy as shown in Fig. 2.

As was mentioned previously, McCombe and Wagner[10] experimentally determined the conduction-band g factor g_c^* from Eq. (4) as a function of magnetic field from spin-resonance measurements. In Fig. 3 their values for $g_c^*(B)$ are plotted along with theoretical results of other work[4,34] and of this study. The theoretical calculation of $g_c^*(B)$ was obtained by finding the theoretical energy difference $\hbar\omega_s(B)$ between the $a(0)$ and $b(0)$ Landau levels of the different theories and then using Eq. (4) to determine $g_c^*(B)$. As shown, the theoretical lines of Pidgeon *et al.*[34] and Johnson and Dickey[4] underestimate and overestimate the data, respectively. The band parameters of this study were adjusted to fit g_c^* to McCombe and Wagner's data.[10] Thus there is good agreement between theory and data even for Isaacson's[27] $B=0$ value of -51.3. The higher band parameter which influences $g_c^*(B)$ the most is N_1, which is -0.55 from these measurements. At $B=0$ our value of $g_c^*(0)$ is -50.6, while Johnson and Dickey's result is $g_c^*(0)=-51.3$. The excellent fit of the theory to $g_c^*(B)$ is also apparent in Fig. 1 where the same good agreement of the transition energies to the spin-resonance line $b(0)$ also occurs. In the same manner Weiler[35] also explained the magnetic field dependence of the spin-flip frequency (ω_s),[10] but with a slightly different set of band parameters.

Phonon-assisted cyclotron-resonance harmonic transitions

Another major magneto-optical effect which is certainly relevant to any discussion of intraconduction processes is that of PACRH. The basic theory for this process was first published by Bass and Levinson.[36] In addition to an electron-photon interaction which causes the processes described in the preceding section, a longitudinal-optical (LO) polar phonon also interacts with the electron-photon system to create absorption resonances. Specifically, an electron in the $a(0)$, spin-up $n=0$, Landau level will absorb a photon, while simultaneously emitting an LO phonon of energy $\hbar\omega_0$, and thus make a transition to some higher n spin-up $a(n)$ Landau level. The simple energy conservation equation for this process is

$$\hbar\omega = n\hbar\omega_c + \hbar\omega_0 = E_a^c(n) - E_a^c(0) + \hbar\omega_0, \tag{8}$$

where $\hbar\omega_0$ is the LO-phonon energy. The transition rate for this process is usually described by second-order perturbation theory[36,37] and can be written as

$$T_{if} = \frac{2\pi}{\hbar}\left|\sum_t \frac{\langle f|H_L|t\rangle\langle t|H_R|i\rangle}{E_t - E_a^c(0) - \hbar\omega} + \sum_{t'} \frac{\langle f|H_R|t'\rangle\langle t'|H_L|i\rangle}{E_{t'} - E_a^c(0) - \hbar\omega_0}\right|^2 \times \delta(E_a^c(n) - E_a^c(0) - \hbar\omega + \hbar\omega_0), \tag{9}$$

where H_R and H_L are the electron-photon and electron-phonon interactions, respectively, and $E_a(0)$, E_t, and $E_a(n)$ are the energies of the initial, intermediate, and final states (i,t,f), respectively. The δ function is a statement of the energy conservation, Eq. (8), and the sum is over all possible intermediate states. For the light polarization σ_L in the electron-photon interaction H_R, the Landau-level number n changes to $n+1$ from the initial to the intermediate states (first term) or intermediate to final states (second term) for the same spin. The electron-phonon interaction H_L allows a transition from a state n to any state n', but is strongly spin conserving. Thus, although there are definite selection rules for the electron-photon interaction, transi-

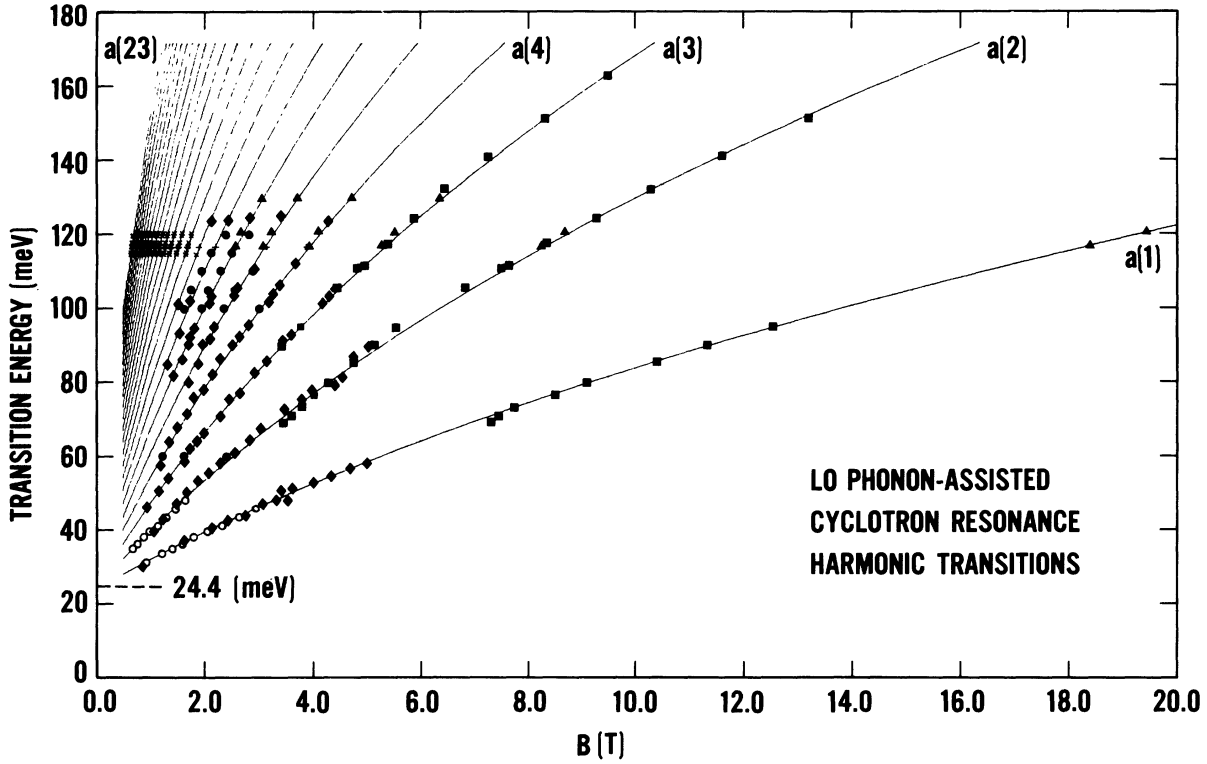

FIG. 4. Fan chart of PACRH for our data and other authors. The labels are the final state of the transition while the initial state is the $a(0)$ Landau level. The intercept corresponds to the LO-phonon energy (24.4 meV). The data points are as follows: ○, Ref. 4; ▲, Ref. 6; ■, Ref. 5; ●, Ref. 13; +, Ref. 14; ◆, Ref. 15. The low field ×'s represent our data presented in this paper. An expanded scale of our low-field work is presented in Fig. 6.

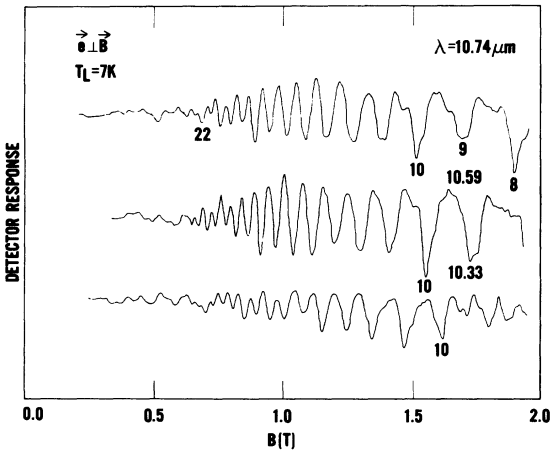

FIG. 5. Wavelength dependence of PACRH. The numbers correspond to distinct experimental transitions.

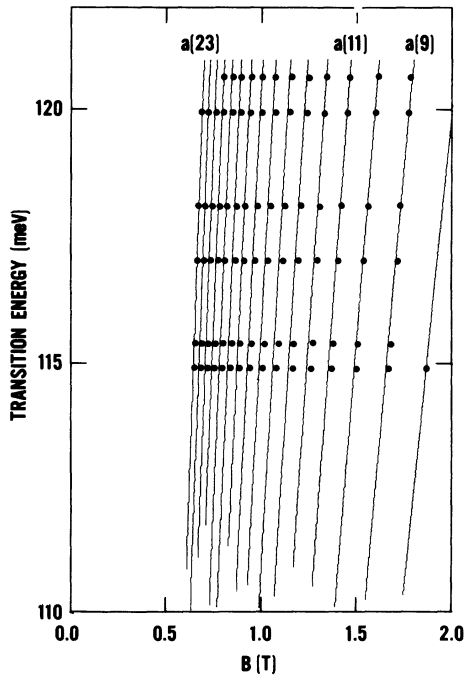

FIG. 6. Expanded scale of the fan chart for PACRH (Fig. 4) with present data. The labels are the final state of the transitions.

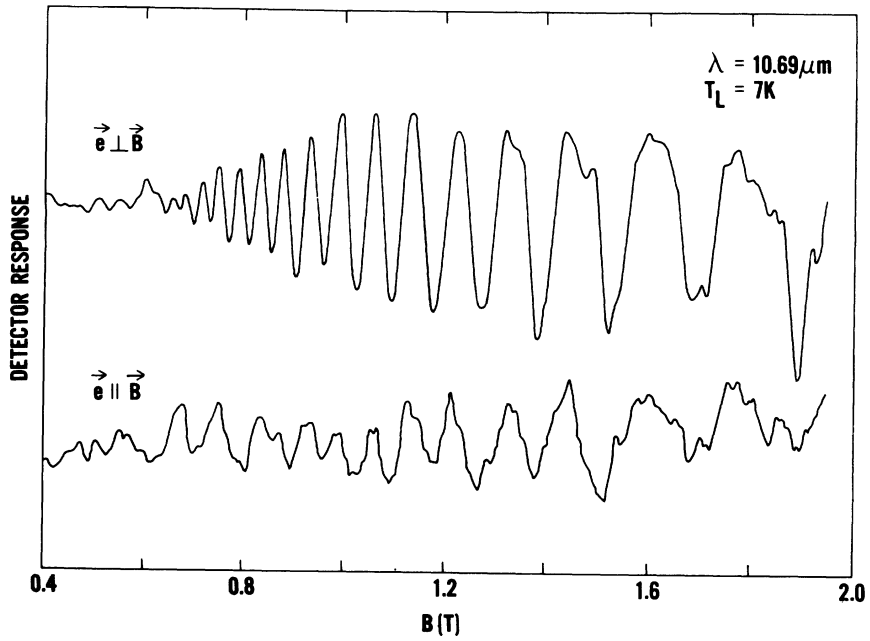

FIG. 7. Polarization dependence of PACRH for $\vec{e}\perp\vec{B}$ and $\vec{e}||\vec{B}$. PACRH is strong for $\vec{e}\perp\vec{B}$ and very weak for $\vec{e}||\vec{B}$.

tions between any Landau levels n and n' are allowed, because there are no selection rules for the electron-phonon interaction. The same types of virtual transitions to and from the intermediate states are also possible for σ_R. PACRH should not be observed for $\vec{e}||\vec{B}$, because then the photon transitions are between states of opposite spin.

The minimum positions of the PACRH structure at each photon energy for new data presented in this paper and the data of other previous work are plotted in Fig. 4. With the set of band parameters determined in this investigation, transition energies for PACRH were also calculated (lines) and compared with the data. In addition to the band parameters already discussed, the LO-phonon energy (the energy intercept at $B=0$) was also used as an adjustable parameter in the computer minimization program. With a fit to all the data shown in Fig. 4, the value

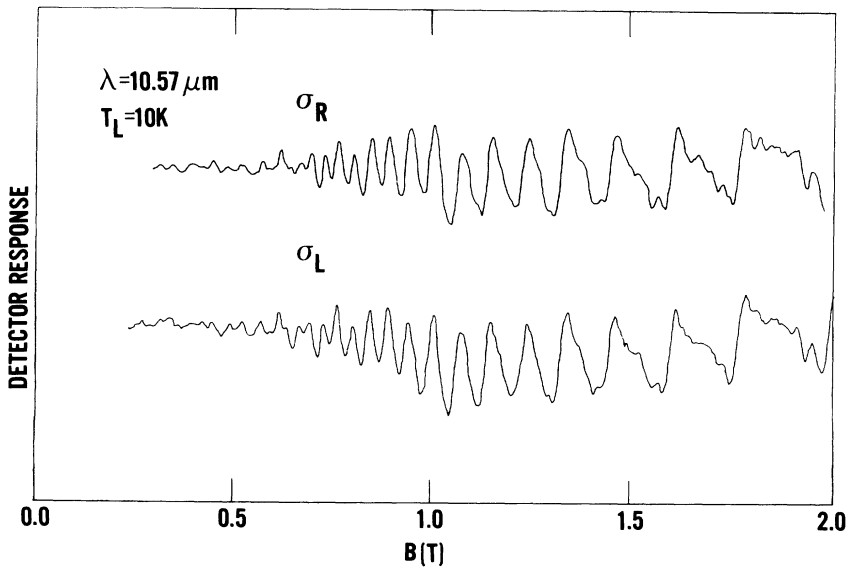

FIG. 8. Polarization dependence of PACRH for σ_R and σ_L. PACRH absorption is equal for both σ_R and σ_L with equal incident powers.

for the LO-phonon energy $\hbar\omega_0$ was found to be 24.4±0.2 meV. Johnson and Dickey[4] also determined the LO-phonon energy from their measurements to be 24.4±0.3 meV. Over the full range of magnetic fields and photon energies there is thus excellent agreement of theory with a wide variety of data using the band parameter set determined in this investigation.

Present results of PACRH

Experiments on PACRH were also performed in this study for n-type-InSb with the free-carrier concentration $\sim 9\times 10^{13}$ cm^{-3}. Figure 5 shows the wavelength dependence of PACRH that we obtained with the sampling and lock-in technique for three representative wavelengths. The PACRH resonances are associated with the minimum structure because the minima correspond to maxima in the conductivity. With the sampling and lock-in technique the detector response is proportional to the second derivative of the photoinduced magnetoresistance. Thus changes in the resistance of the sample are inversely proportional to changes in the conductivity. For PACRH the light induces changes in the mobility of the free electrons in the conduction band, which causes changes in the conductivity of the sample. At a resonance, the light will excite carriers at the bottom of the band to very high energies in the band where the mobility of the carriers is larger, thus increasing the conductivity or decreasing the magnetoresistance. The structure could only be resolved for wavelengths greater than 10.33 μm because two-photon magnetoabsorption[28] dominated the spectra for high photon energies and therefore masked any intra-conduction-band process below that wavelength. The numbers correspond to the Landau-level number of the final state of the transition.

An expanded scale of our low-field data is shown in Fig. 6. The lines represent theoretical calculations using our same set of band parameters, and $\hbar\omega_0=24.4$ meV. With the sensitive sampling and lock-in amplifier technique, transitions to the 23rd harmonic of PACRH can be resolved. Even to these high harmonics of PACRH, our new set of band parameters is still quite valid for describing the observed transition energies.

The polarization dependence of PACRH is shown in Fig. 7 for $\vec{e}\perp\vec{B}$ and $\vec{e}\|\vec{B}$. As indicated, PACRH is much stronger for $\vec{e}\perp\vec{B}$ than for $\vec{e}\|\vec{B}$. The fact that small resonances are even observed for $\vec{e}\|\vec{B}$ is probably due to a small admixture of $\vec{e}\perp\vec{B}$ polarization in the $\vec{e}\|\vec{B}$ trace. In addition to $\vec{e}\perp\vec{B}$ and $\vec{e}\|\vec{B}$ we have also obtained spectra for the circular polarizations σ_R and σ_L, shown in Fig. 8, by propagating the beam through a ZnSe Fresnel rhomb. For both σ_R and σ_L the PACRH resonances appear to have equal strengths. To our knowledge this has not been observed before. However, for the transitions with final states $n=9$–23 in the range of magnetic fields shown here, the transition rate for both σ_R and σ_L are expected to become approximately equal as shown by the following simple argument. For the large harmonics observed here ($n=9$–23) the second sum over t' in the transition probability given in Eq. (9) will dominate, rather than the first sum over t. Thus we consider second-order transitions proceeding by the phonon interaction H_L first and then by the photon interaction for either σ_L or σ_R polarized light. Choosing an intermediate state of Landau-level number $n+1$ for both polarizations allows us to write the transition probability ratio

$$\frac{T^{\sigma_R}_{0,n}(\omega,\omega_c)}{T^{\sigma_L}_{0,n+2}(\omega,\omega_c')}\approx\frac{|\langle n|H_R^{\sigma_R}|n+1\rangle|^2}{|\langle n+2|H_R^{\sigma_L}|n+1\rangle|^2}\,\frac{|\langle n+1|H_L^{\sigma_R}|0\rangle|^2}{|\langle n+1|H_L^{\sigma_L}|0\rangle|^2}. \tag{10}$$

The use of Eq. (9) of Ref. 13 to evaluate the photon matrix elements and approximating the ratio of the phonon matrix elements for large n as ~ 1 allows us to write the ratio as $(n+1)/(n+2)$ for a fixed ω. Thus, for large n, the absorption strengths for σ_R and σ_L would not be expected to differ much, as shown in Fig. 8.

CONCLUSIONS

In conclusion we have been able to characterize the conduction band of InSb to much greater accuracy that has previously been reported. With the following set of band parameters, $E_g=235.2$ meV, $E_p=23.2$ eV, $\Delta=0.803$ eV, $\gamma_1=3.25$, $\gamma_2=-0.2$, $\gamma_3=0.9$, $\kappa=-1.3$, $F=-0.2$, $q=0.0$, $N_1=-0.55$, and a modified Pidgeon and Brown Hamiltonian model of the Landau levels, we are able to calculate transition energies for most of the important intra-conduction-band magneto-optical processes. These include cyclotron resonance, combined resonance, cyclotron-resonance harmonics, combined resonance harmonics, electron-spin resonance, and phonon-assisted cyclotron-resonance harmonics (PACRH). In addition, the magnetic field dependence of the conduction-band g_c^* factor is calculated from these band parameters and is found to agree very well with the experimental spin-resonance results.[10,11,27]

It should also be noted that these band parameters can also be used to calculate transition energies that are also in excellent agreement with recent intra-valence-band[29] and two-photon-interband[28] magneto-optical data. Except for the value of E_g, these band parameters are in good agreement with those obtained by Weiler[35] from analyzing one-photon-interband data, including exciton contributions. Thus with one band-parameter set more magneto-optical processes can now be explained, making this the most accurate set for InSb so far.

In addition to the band-parameter studies we also present new experimental results of PACRH. With a sensitive photoconductivity technique PACRH transitions up to the 23rd harmonic have been resolved, extending previous observations of PACRH to much lower magnetic fields ($B \simeq 6$ kG). From polarization studies PACRH is shown to be present for $\vec{e} \perp \vec{B}$, but almost absent for $\vec{e} \| \vec{B}$, as expected. However, polarization measurements with circularly polarized light (σ_R and σ_L) indicate that, at least in the magnetic field range of our experiments PACRH absorption is approximately equal for both σ_R and σ_L, in agreement with simple predictions.

ACKNOWLEDGMENTS

This work was supported in part by the U.S. Office of Naval Research and a Faculty Research Grant from North Texas State University. We gratefully acknowledge the help and support of M. W. Weiler, whose energy-band model was used extensively in this study.

*Present address: Texas Instruments, Inc., Dallas, Texas 75265.

[1]C. R. Pidgeon and R. N. Brown, Phys. Rev. 146, 575 (1966).
[2]B. D. McCombe, S. G. Bishop, and R. Kaplan, Phys. Rev. Lett. 18, 748 (1967).
[3]B. D. McCombe, Phys. Rev. 181, 1206 (1969).
[4]E. J. Johnson and D. H. Dickey, Phys. Rev. B 1, 2676 (1970).
[5]K. Lee, B. S. thesis, Massachusetts Institute of Technology, 1976 (unpublished).
[6]R. Grisar, H. Wachernig, G. Bauer, J. Wlasak, J. Kowalski, and W. Zawadzki, Phys. Rev. B 18, 4355 (1978).
[7]H. Wachernig, R. Grisar, G. Bauer, and S. Hayashi, Physica 89B, 290 (1977).
[8]M. H. Weiler, R. L. Aggarwal, and B. Lax, Solid State Commun. 14, 299 (1974).
[9]M. H. Weiler, R. L. Aggarwal, and B. Lax, Phys. Rev. B 17, 3269 (1978).
[10]B. D. McCombe and R. J. Wagner, Phys. Rev. B 4, 1285 (1971).
[11]F. Kuchar, R. Meisels, and M. Kriechbaum, in the *Proceedings of the Physics of Narrow Gap Semiconductors, Linz, Austria, 1981,* edited by E. Gornik, H. Heinrich, and L. Palmetshofer (Springer, New York, 1982), p. 197.
[12]G. Bemski, Phys. Rev. Lett. 4, 62 (1960).
[13]R. C. Enck, A. L. Saleh, and H. Y. Fan, Phys. Rev. 182, 790 (1969).
[14]S. Morita, S. Takano, and H. Kawamura, J. Phys. Soc. Jpn. 39, 1040 (1975).
[15]V. I. Ivanov-Omskii, K. I. Korovin, and E. M. Shereghii, Phys. Status Solidi B 90, 11 (1978).
[16]C. R. Pidgeon and S. H. Groves, Phys. Rev. 186, 824 (1969).
[17]M. H. Weiler, Ph.D. thesis, Massachusetts Institute of Technology, 1977 (unpublished).
[18]G. Dresselhaus, A. F. Kip, and C. Kittel, Phys. Rev. 48, 368 (1955).
[19]G. Dresselhaus, A. F. Kip, C. Kittel, and G. Wagoner, Phys. Rev. 98, 556 (1955).
[20]E. Burstein, G. S. Picus, and H. A. Gebbie, Phys. Rev. 103, 825 (1956).
[21]R. J. Keyes, S. Zwerdling, S. Foner, H. H. Kolm, and B. Lax, Phys. Rev. 104, 1804 (1956).
[22]H. Lipson, S. Zwerdling, and B. Lax, Bull. Am. Phys. Soc. 3, 218 (1958).
[23]E. D. Palik, G. S. Pikus, S. Teitler, and R. F. Wallis, Phys. Rev. 122, 475 (1961).
[24]R. L. Bell and K. T. Rogers, Phys. Rev. 152, 746 (1966).
[25]R. B. Dennis, R. A. Wood, C. R. Pidgeon, S. D. Smith, and J. W. Smith, J. Phys. C 5, L73 (1972).
[26]G. Favrot, R. L. Aggarwal, and B. Lax, Solid State Commun. 18, 577 (1976).
[27]R. A. Isaacson, Phys. Rev. 169, 312 (1968).
[28]M. W. Goodwin, D. G. Seiler, and M. H. Weiler, Phys. Rev. B 15, 6300 (1982).
[29]C. Littler, D. G. Seiler, R. Kaplan, and R. J. Wagner (unpublished).
[30]R. L. Aggarwal, in *Semiconductors and Semimetals,* edited by R. K. Willardson and A. C. Beer (Academic, New York, 1972), Vol. 9, p. 151.
[31]J. Apel, T. Poehler, and C. Westgate, Appl. Phys. Lett. 14, 161 (1969).
[32]C. Summers, R. Dennis, B. Wherrett, P. Harper, and S. Smith, Phys. Rev. 170, 755 (1968).
[33]B. McCombe, Solid State Commun. 6, 533 (1968).
[34]C. R. Pidgeon, D. L. Mitchell, and R. N. Brown, Phys. Rev. 154, 737 (1967).
[35]M. H. Weiler, J. Magn. Magn. Mater. 11, 131 (1979).
[36]F. G. Bass and I. B. Levinson, Zh. Eksp. Teor. Fiz. 49, 914 (1965) [Sov. Phys.—JETP 22, 635 (1966)].
[37]W. Zawadski, in *Proceedings of the Narrow Gap Semiconductors Physics and Applications, Nimes 1979,* Vol. 133 of *Lecture Notes in Physics,* edited by W. Zawadzki (Springer, New York, 1980), p.85.